Early-Life Commensal Lung Bacteria Shape Immune Responses and RSV Susceptibility in Neonatal Mice

Quentin Marquant[§1,2], Claire Chottin[§1], Cécile Ferret[1], Eloi Poucet[1], Vinciane Saint-Criq[3], Daphné Laubreton[1], Carole Drajac[1], Edwige Bouguyon[1], Aude Remot[4], Samuel Constant[5], Song Huang[5], Edouard Sage[1,2], Isabelle Schwartz-Cornil[1], Muriel Thomas[3], Sabine Riffault[1], and Delphyne Descamps[¶1]

[§]Equal contribution

[¶]Corresponding author

[1]Université Paris-Saclay, INRAE, UVSQ, VIM, 78350, Jouy-en-Josas, France

[2]Hôpital Foch, Suresnes, France

[3]Université Paris-Saclay, INRAE, Micalis, 78350, Jouy-en-Josas, France

[4]Université de Tours, INRAE, ISP, 37380, Nouzilly, France

[5]Epithelix, 18, Chemin des Aulx, CH-1228 Plan-les-Ouates, Geneva, Switzerland

Correspondence to: Delphyne Descamps, Tel: (33) 01 34 65 26 10, Email: delphyne.descamps@inrae.fr. Virologie et Immunologie Moléculaires, INRAE, UVSQ, Domaine de Vilvert, 78350 Jouy-en-Josas, France.

Abbreviations

RSV: respiratory syncytial virus; LTRI: lower respiratory tract infections; ILC2: type 2 innate lymphoid cells; AM: alveolar macrophages; IFN-I: type 1 interferons; ISG: interferon-stimulated genes; EL-Abx: early-life antibiotic treatment; BHI: Brain Heart Infusion; MRS: Man Rogosa Sharpe; PCLS: Precision-cut lung slices; CFU: colony forming unit; MOI: multiplicity of infection; BAL: Bronchoalveolar lavage; LDH: lactate deshydrogenase; i.n.: intranasal; MGG: May-Grunwald-Giemsa.

Acknowledgements

We greatly acknowledge M. Prost and A. Mialet for their assistances with experiments. We are grateful to M-A. Rameix-Welti (INSERM, U1173, UVSQ) and J-F Eléouët (INRAE, UVSQ, VIM) for providing recombinant RSV-Cherry. We are grateful to the IERP unit, INRAE (Infectiology of

fishes and rodent facility, doi: 10.15454/1.5572427140471238E12). We thank the Emerg'in platform for access to IVIS-Spectrum that was financed by the Region Ile De France (DIM One Health). We thank E Helloin and C Darrigo (CIRM, INRAE, Nouzilly) for bacterial strains identification by mass spectrometry. C. Drajac. and Q. Marquant were the recipient of a Ph.D. and post-doctoral fellowships of Région Ile-de-France (DIM-Malinf or DIM-OneHealth, respectively). C. Chottin was the recipient of a Ph.D. fellowship from the French research ministry. D. Laubreton and experiments were supported by a grant of the French national research agency "Agence Nationale de la Recherche" (ANR-13-BSV3-0016 and ANR-24-NEOMIS). This project was supported by the Fondation Air Liquide, Vaincre la Mucoviscidose and by Association Grégory Lemarchal.

Conflict of Interest statement

The authors declare no competing financial interests. The authors declare that all the other data supporting the findings of this study are available within the article and its supplementary information files and from the corresponding author upon request.

Sample Credit author statement

Quentin Marquant: Methodology, Validation, Investigation, Data curation, Visualization, Writing – review & editing. **Claire Chottin:** Methodology, Validation, Investigation, Data curation, Visualization, Writing – review & editing. **Cécile Ferret:** Validation, Data curation, Resources. **Eloi Poucet:** Validation, Data curation. **Vinciane Saint-Criq:** Methodology, Writing – review & editing. **Edwige Bouguyon:** Validation, Data curation. **Daphnée Laubreton:** Methodology, Investigation, Writing – review & editing. **Carole Drajac:** Methodology, Investigation. **Aude Remot:** Methology, Conceptualization. **Samuel Constant:** Resources. **Song Huang:** Resources. **Edouard Sage:** Resources. **Isabelle Schwartz-Cornil:** Resources, Conceptualization, Writing – review & editing. **Muriel Thomas:** Resources, Conceptualization, Funding acquisition, Writing – review & editing. **Sabine Riffault:** Conceptualization, Funding acquisition, Writing – review & editing. **Delphyne Descamps:** Conceptualization, Methodology, Investigation, Validation, Formal analysis, , Writing – Original Draft, Writing – review & editing, Supervision, Visualization, Project administration, Funding acquisition.

Abstract

The lung mucosa at birth and shortly after is particularly vulnerable to respiratory syncytial virus (RSV) infection. Respiratory disease severity is strongly influenced by the age at first exposure, which may also affect the trajectory of airway function. Early-life represents a critical window for lung development and initial microbiota colonization, both of which shape mucosal immune responses to RSV. The impact of the initial establishment of the lung microbiota by its primo-colonizing strains on susceptibility to RSV infection remains largely unknown. In the present study, we showed that early-life primo-colonizing bacterial strains in the mouse lung differentially induce innate immune responses and influence RSV susceptibility in *ex vivo* models using lung explants and alveolar macrophages. We identified a specific bacterial strain that enhances IFN-I antiviral pathways and reduces RSV replication both *in vitro* and *in vivo*. Intranasal administration of this strain to neonatal mice prevented the development of immunopathological responses upon RSV reinfection in adulthood. These findings highlight the potential of early-life microbiota modulation as a promising intervention for preventing RSV disease and its long-term respiratory consequences.

Keywords

Respiratory Syncytial Virus (RSV), Early-life, Lung microbiota, Primo-colonizing bacteria, Mucosal immunity, Immune imprinting, Interferon, Alveolar macrophages, lung explants

81 **Research article**

82 **Introduction**

83 The respiratory syncytial virus (RSV), known as the primary cause of bronchiolitis in infants, is a
84 major contributor to lower respiratory tract infections (LRTIs), and remains the leading cause of child
85 mortality worldwide[1]. Moreover, severe RSV infection in early-life has been associated with long-
86 term respiratory problems, such as repeated LRTI, wheezing, asthma, and reduced lung function,
87 which can continue into adulthood in the form of chronic respiratory disease[2]. New passive
88 immunisation strategies, such as maternal vaccination or administration of monoclonal antibodies,
89 have been approved to reduce the burden of acute RSV infection in high-risk infants. However, some
90 complications have been reported, including an increase in preterm births[3]. Direct vaccination in
91 children remains a challenge, particularly after the FDA recently suspended all RSV vaccine trials in
92 infants following reports of increased cases of severe illness in one trial[4]. The mechanisms underlying
93 pulmonary hypersensitivity to RSV in early-life and its long-term health effects remain to be
94 elucidated in order to develop effective prophylactic strategies. An increasing number of studies on
95 RSV-infected neonatal mice (less than 7 days old at initial infection) have validated this model as
96 relevant for understanding RSV infection in human infants[5]. It has been shown that the age at first
97 infection plays a key role in shaping subsequent immune responses, notably by inducing epigenetic
98 modifications[6]. This may increase the severity of later RSV infections[7], potentially by driving a type
99 2-biased immunity[8], which promotes allergic responses later in life[6]. Moreover, the early-life in mice
100 is characterized by an immediate permissiveness to RSV replication, which gradually decreases with
101 age as the ability to mount type I interferon (IFN-I) responses improves[9]. IFN-I are rarely detected in
102 nasal washes from RSV-infected children[10]. However, IFN-α and IFN-β control viral pathogenesis
103 by inducing interferon-stimulated genes that provide an early antiviral defense and shape
104 inflammatory and adaptive immune responses[11]. IFN-I responses appear to play a key role in the
105 outcome of RSV infection[11], as treatments that enhance IFN-I levels in infected neonatal mice have
106 been shown to reduce viral replication and long-term RSV-induced lung effects[12, 13]. Thus,
107 modulation of pulmonary innate immune defenses during the perinatal period can affect susceptibility
108 to RSV infection, and determine long-term respiratory outcomes.

109 Early-life is indeed a crucial period for lung mucosa development, during which
110 environmental factors influence the maturation of three interconnected components, namely, the
111 airway epithelium, immune cells, and the resident microbiota. When the tuning between these three
112 components is inadequate, it can ultimately affect susceptibility to infections or predispose to chronic
113 respiratory diseases[14]. There is increasing evidence that postnatal lung mucosa is biased toward a type
114 2 immune response, as indicated by the spontaneous accumulation of type 2 innate lymphoid cells

115 (ILC2), eosinophils, and basophils, along with the production of cytokines such as IL-33 and IL-13[15],
116 which are typically involved in anti-inflammatory responses and tissue repair. Such a tissue
117 environment is prone to the early polarization of tissue-resident alveolar macrophages (AMs) toward
118 a tolerogenic, anti-inflammatory M2 phenotype[16]. Moreover, the lung microbiota establishes rapidly
119 after birth and it shaped by factors linked to the host and the environment[17, 18, 19]. A recent prospective
120 pediatric cohort study showed that between birth and 3 months of age, rapid changes in the airway
121 bacterial microbiota are accompanied by a major shift in the JAK/STAT and interferon immune
122 pathways, revealing a link between bacterial communities and early-life respiratory immunity[20]. In
123 addition, the lung microbiota contributes to immune tolerance in early-life according to an asthma
124 model[17] and attenuates innate immune reactivity to PAMPs[21].

125 The incidence of respiratory infections and the occurrence of dysbiosis in the lung microbiota
126 are closely related[22]. The severity of RSV infection,[23, 24] and the persistence of symptoms in children
127 may be influenced by the bacterial ecosystem[25]. Conversely, the presence of *Lactobacillus* in the
128 nasopharynx is associated with a reduced risk of childhood wheezing illnesses at 2 years of age[26]. In
129 mice, viable commensal bacteria are detected in the lungs as early as 3 days of age, with their number
130 and diversity increasing over time[17] and reaching a plateau by weaning at around 21 days of age[19]. A
131 collection of primo-colonizing bacteria was established *via* their isolation from lung homogenates of
132 neonatal mice using aerobic or anaerobic culture conditions[19]. Intranasal administration of certain
133 strains of this collection during early life influenced the outcome of an allergic asthma model[19], while
134 instillation of other strains in adult mice attenuated pulmonary inflammation following
135 *Mycobacterium tuberculosis* infection[27]. These findings suggest that lung primo-colonizing
136 commensal bacteria can modulate pulmonary immunity and influence susceptibility to respiratory
137 diseases. However, the mechanisms by which early bacterial colonization of the lungs modulates
138 immune responses and determines both immediate and long-term respiratory outcomes, including
139 during early-life RSV infection, remain largely unexplored[28]. In the present study, we demonstrated
140 that early-life commensal lung bacteria modulate immune responses and RSV susceptibility in
141 neonatal mice. We established a proof of concept demonstrating that it is possible to select a single
142 strain from a panel of lung primo-colonizing commensal bacteria based on its immunomodulatory
143 and antiviral properties on the neonatal lungs. One bacterial strain in particular, hereafter referred to
144 as strain 17, promoted IFN-I antiviral pathways and reduced RSV replication both *in vitro* and *in*
145 *vivo*. Finally, its intranasal administration to neonatal mice prevented early-life immunopathological
146 priming, which became apparent after a second exposure to RSV in adulthood.

147 **Materials and methods**

148 ***Mice***

149 Pregnant BALB/cJrj mice were purchased from Janvier (Le Genest, France). All experiments were
150 approved by the ethics committee COMETHEA (Ethical Committee for Animal Experimentation,
151 authorization number: APAFIS#14654-2018032116445169).

152 ***Bacterial strains' identification and growth***

153 Bacterial strains (Supplemental Table 1) previously isolated from 3-day-old mouse lungs were stored
154 at −80°C[19]. Strains were revived in 10 mL yeast-heminBHI or MRS medium and subcultured (100
155 µL/10 mL). Growth was monitored hourly for 8h by spectrophotometry to determine exponential and
156 stationary phases. Bacterial counts were obtained using a BD Accuri™ C6 flow cytometer, and strain
157 identity was confirmed by 16S PCR (J4/J7 primers) and MALDI-TOF mass spectrometry (CIRM,
158 INRAE, Nouzilly, France).

159 ***Virus***

160 Human RSV strain A2 and recombinant RSV-Long expressing mCherry (RSV-mCherry) or
161 luciferase (RSV-Luc) were produced, titrated on HEp-2 cells, and stored at -80°C[29].

162 ***Ex vivo lung explants, stimulation and infection***

163 Lungs from 6-day-old neonatal mice were filled *via* tracheotomy with RPMI containing 1.5% low-
164 melting agarose (37°C). After solidification, lungs were placed in a Krumdieck tissue slicer
165 (MD6000) chamber containing PBS with 1× antibiotic-antimycotic and cut into 150 µm slices to
166 obtain precision-cut lung slices (PCLS)[19, 21]. PCLS were stimulated for 16h at 37 °C, 5% CO_2 with
167 strains (50 CFU/well in RPMI with 5% FBS and L-glutamine). Inoculations were verified by CFU
168 counts on agar plates. Three hours later, PCLS were infected with RSV-Luc (7.19×10^4 PFU/well)
169 or Mock control. Supernatants were collected. PCLS were lysated in lysis buffer (5 mM EDTA, 150
170 mM NaCl, 50 mM Tris-HCl, 1% Triton X100, pH 7,4) or Passive Lysis Buffer (30 mM Tris, 10 mM
171 $MgCl_2$, 1% Triton 100X, 2% Glycerol) using a Precellys 24-bead grinder homogenizer (Bertin
172 Technologies) for 2 × 15s at 6,000 x g. Protein levels were quantified with DC™ or RC-DC™ Protein
173 Assays (Bio-Rad).

174 ***Experiments with differentiated human primary bronchial epithelial cells***

175 MucilAir® from healthy donors were purchased from Epithelix. Cells (≈5 x 10^5 cells/transwell) were
176 stimulated with bacterium 17 (10^3 CFU/transwell) in 20 µL in apical side. After 3h, cells were
177 infected with RSV-mCherry (MOI = 0.1) or Mock control during 3h. The inoculum was removed and
178 medium replaced by strain 17 containing fresh medium. RSV-mCherry replication was visualized
179 using the ZOE Fluorescent Cell Imager (Bio-Rad) and quantified with a fluorescence plate reader
180 (Tecan Infinite 200 Pro). Supernatants and cell lysates were then collected.

181 ***Ex vivo AM culture and infection***

182 Bronchoalveolar lavages (BALs) were performed on 6-days-old mice to isolate AM, as previously
183 described[9, 30, 31]. Cells (1 x 10^5) were plated, 24h after seeding, incubated with bacterial strains (50
184 CFU/well) for 3h before exposure to RSV-Long (MOI = 5) or a mock control. Supernatants and cells
185 were collected 24h post-infection.

186 ***Cell cytotoxicity***

187 Cytotoxicity was measured by lactate deshydrogenase (LDH) activity, using the Non-Radioactive
188 Cytotoxicity Assay kit (Promega).

189 ***Cytokine, IFN, and RSV-specific Ab assays***

190 Cytokine production was measured using the 15-plex or IL-6/TNF-α/IFN-α/IFN-β custom 4-Plex
191 mouse ProcartaPlex™ immunoassay (ThermoFisher Scientific). Human IL-6, TNF-α or IP-10 were
192 measured by Luminex and human β-defensin-2 by ELISA (NB-50-1634-1000, NeoBiotech). Data
193 were read on MagPix instrument (Luminex), and analyzed using Bio-Plex Manager software (Bio-
194 Rad). HEK-Blue™ IFN-λ (InvivoGen) cells were used for the detection of bioactive human IFN-λ.
195 Individual mouse sera were assayed for specific Ab (IgG1, IgG2a) against RSV lysates by ELISA[13].

196 ***In vivo bacterial strains inoculation and RSV infection***

197 Neonate mice (age 3 and 5 days) received 10 µL of strain 17 intranasally (i.n.) route. At 6 days old,
198 mice were infected with RSV-Luc (7.187 x 10^6 PFU/mL, 10 µL, i.n) or a Mock control. In other
199 experiments, neonate mice were first infected by RSV-A2 (2.3 × 10^6 PFU/mL, 10 µL, i.n.), and were
200 kept until 8 weeks of age when they were all infected with RSV-A2 (100 µL, i.n.)[13]. BAL and lung
201 tissues were collected.

202 ***Bioluminescence measurements***

203 Photon emission was measured in lysates of the nasal cavity or lung tissues and PCLS using the IVIS
204 system (Xenogen Biosciences) and Living Image software (version 4.0, Caliper Life Sciences),
205 following a previously described method[9], and was normalized to protein content.

206 ***Cell infiltration***

207 Cells were collected from BALs and centrifugated at 400 x g for 10min at 4°C. May-Grunwald-
208 Giemsa coloration was performed to assess the differential cell counts using light microscopy. Two
209 hundred cells were counted to determine relative and absolute cell numbers.

210 ***RT-qPCR***

211 Total RNA was extracted from lung lysates using a NucleoSpin® RNA midi column (Macherey
212 Nagel) and reverse transcribed using random primers and SuperScript II (Invitrogen), according to
213 the manufacturer's instructions. The primers (Sigma–Aldrich) used are listed (**Supp. Table 2**). RT-
214 qPCR was performed in duplicate for each gene using the CFX Connect™ Real-Time PCR Detection

System (Bio-rad) and SYBRGreen PCR Master Mix (Eurogenetec). Data were analyzed using CFX Manager™ Software (Bio-rad) to determine the quantification cycle (Cq) values. Results were determined using the formula $2^{-\Delta Cq}$, with $\Delta CQ = Cq_{gene} - Cq_{(mean\ (bActine, Gapdh, Hprt))}$.

Data and statistical analysis

Data are expressed as mean ± SEM. Statistical significance was set at $*P < 0.05$, $**P < 0.01$, $***P < 0.001$, and $****P < 0.0001$ using GraphPad Prism 8 (GraphPad Software Inc.). Data normality was assessed using the D'Agostino–Pearson and Shapiro–Wilk tests. Depending on the distribution, differences between groups were analyzed using a parametric *t*-test or a nonparametric Mann–Whitney test (two groups), or by one-way ANOVA/Kruskal–Wallis or two-way ANOVA with Tukey's multiple comparisons test.

226 **Results**

227 **Primo-colonizing bacteria exert distinct immunostimulatory effects on neonatal lung mucosa**
228 ***ex vivo* model.**

229 The goal was to challenge the concept that a strain capable of promoting a protective type 1 immunity
230 in the lungs during early-life. To evaluate the immunostimulatory effects of primo-colonizing
231 bacterial strains (**Supp. Table 1**) on the neonatal lung, we established a PCLS-based screening assay
232 using lung tissue from 6-day-old mice, an *ex vivo* model that recapitulates pulmonary cytokine
233 production[32]. PCLS were exposed to each strain at MOI=50 (**Fig. 1A**). Among 20 strains tested, two
234 (strains 1 and 11) caused significant cytotoxicity after 16h and were excluded, while most showed
235 cytotoxicity levels comparable to the control medium (mean = 21.3% ± 1.1%), indicating no harmful
236 effects (**Supp Fig. 1A**). Cytokines were quantified using a 15-plex assay and grouped by functional
237 category (pro-inflammatory, type 1 immunity, type 2 immunity, Th17/Th22/Th9-responses, and
238 lymphocyte proliferation, **Supp. Fig. S1B-E**). Both the nature and magnitude of cytokine production
239 by PCLS varied across bacterial strains. Strains 2, 19 and 16 induced high levels of pro-inflammatory
240 cytokines such as TNF-α and IL-6, together with robust a type 2 immune response, including IL-10
241 (**Supp. Fig. S1B and D**). In contrast, most other strains induced low cytokine production. A bacterial
242 strain, the strain 17, stood out from the others. Strain 17, identified as *Escherichia coli* by 16S
243 sequencing and mass spectrometry (**Supp. Table 1**), also inducing type 2 cytokines (**Supp. Fig. S1D**)
244 but was unique in triggering a strong type 1 profile, characterized by a high production of IFN-γ and
245 IL-12p70 (**Fig. 1B**), and increased IL-22 and IL-9 secretion (**Supp. Fig. S1E**). To highlight strain-
246 specific immune signatures, cytokine levels were expressed as fold-change relative to control PCLS
247 and visualized as heat map (**Fig. 1C**), with hierarchical clustering revealing groups of strains with
248 similar immunostimulatory patterns. Overall, primo-colonizing lung bacteria displayed distinct
249 immunostimulatory capacities in PCLS from neonatal mice, with strain 17 standing out for its
250 strongly type 1-skewed immune profile and lack of cytotoxicity.

251 **Strain 17 treatment of neonates attenuates the long-term pulmonary consequences of early-life**
252 **RSV infection upon rechallenge in adulthood.**

253 *In vitro*, bacterial strain 17 demonstrated a pronounced enhancement of type 1 immune responses. To
254 assess the *in vivo* relevance of its effect, we first investigated whether intranasal (i.n.) administration
255 of strain 17 (10^6 CFU; dose and method previously shown to deliver sufficient bacteria to the lungs[19])
256 was pathogenic in neonatal mice. No mortality was observed in neonatal mice following
257 administration of strain 17 (data not shown). A modest elevation in neutrophil counts was detected in
258 BALs, although total cell numbers remained unchanged (**Fig. S2**). Thus, we employed a previously
259 described model of adult RSV re-exposure to investigate the ability of strain 17 to promote protective

260 immunity and counteract early-life immunopathological priming[8]. Three-day-old mice were treated
261 intranasally with strain 17 or PBS vehicle at days 3, 5, 8, and 10 days of age. At 6 days old, mice
262 were infected intranasally with RSV, followed by a second exposure in adulthood (**Fig. 2A**). Weight
263 change was monitored (**Fig. 2B**), and antibody responses (**Fig. 2C-D)** and cell infiltration in BALs
264 were assessed (**Fig. S3B-E**). As expected, mice initially infected as pups and re-exposed to RSV in
265 adulthood (PBS/RSV/RSV group) lost weight for over the 14 days post-infection (d.p.i), whereas
266 mice treated with strain 17 and infected with RSV as neonates (strain 17/RSV/RSV group) lost little
267 weight and regained their initial weight by 8 d.p.i., consistently showing a better although not
268 stastically significant, maintenance of body weight compared with controls (**Fig. 2B**). We next
269 investigated whether neonatal strain administration would impact the anti-RSV IgG1 response
270 indicative of type 2 immunity and expected for adults upon RSV reexposure[8]. As expected, the re-
271 exposure to RSV in adulhood induced a significant production of anti-RSV-IgG1 at 14 d.p.i. in the
272 PBS/RSV/RSV group (**Fig. 2C**). In contrast, strain 17-treated neonates showed an early induction of
273 anti-RSV-IgG2a antibody production as soon as 7 d.p.i. (**Fig. 2D**) and no significant increase in IgG1
274 at 14 d.p.i. (**Fig. 2C**). Finally, we monitored cellular inflammation. At 7 d.p.i., total BAL cell numbers
275 were significantly higher in mice first infected as neonates and re-exposed as adults (PBS/RSV/RSV,
276 $2.51 \times 10^5 \pm 0.38 \times 10^5$ cells) than in mice infected only as adults (PBS/Mock/RSV, $1.26 \times 10^5 \pm 0.33$
277 $\times 10^5$ cells ; **Fig. S3B**, $p < 0.05$). BAL cell counts in strain 17/RSV/RSV-treated mice did not differ
278 significantly from the PBS/RSV/RSV group (**Fig. S3B**). Macrophage and neutrophil numbers were
279 similar across groups at 7 and 9 d.p.i. (**Fig. S3C–D**), while the overall leukocyte increase was mainly
280 due to lymphocyte recruitment ($0.98 \times 10^5 \pm 0.19 \times 10^5$ cells in PBS/RSV/RSV *vs.* $0.81 \times 10^5 \pm 0.24$
281 $\times 10^5$ cells in strain 17/RSV/RSV; **Fig. S3E**), which persisted until 9 d.p.i. despite declining over
282 time. Significant eosinophil recruitment was observed in the BAL of PBS/RSV/RSV mice at 7 d.p.i.
283 ($0.08 \times 10^5 \pm 0.012 \times 10^5$ cells) and persisted at 9 d.p.i. ($0.065 \times 10^5 \pm 0.019 \times 10^5$ cells), but was
284 absent in PBS/Mock/RSV mice, reflecting type 2 immune priming from early-life RSV infection
285 (**Fig. 2E–F**). Notably, eosinophil infiltration was nearly abolished in mice treated with strain 17 prior
286 to the first RSV infection ($0.006 \times 10^5 \pm 0.004 \times 10^5$ cells at 7 d.p.i.). Accordingly, the strain
287 17/RSV/RSV group had 9.6- and 3.4-fold fewer eosinophils in the BAL compared to PBS/RSV/RSV
288 animals at 7 and 9 d.p.i., respectively. Neonatal treatment with strain 17 did not affect overall
289 leukocyte infiltration upon adult RSV re-exposure but prevented immunopathologic eosinophilia.
290 Altogether, these data indicate that the early-life presence of strain 17 during the first RSV infection
291 of mice promoted a shift in the RSV-specific antibody toward a type 1 profile (higher IgG2a, lower
292 IgG1), associated with minimal eosinophil recruitment and improved disease outcomes (trend to
293 maintain their weight).

294 **Exposure to strain 17 reduces RSV replication in PCLS.**

295 We next focused on the early events following RSV infection to explore how strain 17 affects early
296 innate antiviral response. To assess whether strain 17 influences early-life RSV susceptibility, we
297 performed co-exposure experiments using PCLS from 6-day-old mice. PCLS were first exposed to
298 strain 17 (50 CFU/well as previously used[19]) to elicit its immunostimulatory effects, and then infected
299 with luciferase-expressing RSV (RSV-Luc) or mock-treated for 16h to evaluate viral replication (**Fig.**
300 **3A**). Strains 16, 24, and 25, displaying distinct cytokine profiles (**see Fig. S1**), were included as
301 comparators. Cytotoxicity induced by these strains, RSV-Luc, or their combination did not exceed
302 21% and was comparable to that of the control medium. Thus, co-exposure did not affect PCLS
303 viability and supporting the safe use of these bacteria during RSV infection (**Fig. 3B**). Viral
304 replication was quantified in PCLS lysates using a luciferase activity assay (**Fig. 3C**). PCLS exposed
305 to strain 25 showed a slight increase in luciferase activity compared to the control condition (not
306 statistically different), suggesting a potential enhancement of RSV replication associated with the
307 presence of strain 25. Pre-exposure to strains 16 or 24 resulted in only a slight reduction in RSV
308 replication (non stastistically significant). In contrast, exposure to strain 17 resulted in a strong
309 significant reduction in luciferase activity compared to both control and PCLS exposed to strain 16
310 or 24 conditions. Altogether, these results suggest that pre-exposure to lung primo-colonizing
311 commensal bacteria can modulate RSV replication in PCLS from 6-day-old mice, with strain 17
312 emerging as the most effective strain in reducing RSV replication.

313 **Exposure to strain 17 enhances the innate immune response of neonatal AM to RSV infection.**

314 We also investigated the effect of strain 17 on AMs, the main pulmonary resident immune cells,
315 involved in IFN-I production during RSV infection[33]. AMs isolated from BAL of 6-day-old mice
316 were first exposed to strain 17 (50 CFU/well as previously used[19]) or control medium, followed by
317 exposure to RSV (**Fig. 4A**). After 16h of incubation, exposure of AMs to strain 17 alone induce a
318 slight but unsignificant production of IL-6, TNF-α, and IFN-I in the supernatants compared to basal
319 control conditions (no strain, no RSV, **Fig. 4B-C**). When AMs exposed to strain 17 were subsequently
320 infected with RSV, they produced markedly more inflammatory (IL-6 and TNF-α, **Fig. 4B**) and
321 antiviral (IFN-α and IFN-β, **Fig. 4C**) cytokines than RSV-infected AMs without bacterial pre-
322 exposure. Notably, RSV-infected AMs produced 3-fold higher levels of IFN-I when exposed to strain
323 17. Thus, neonatal AMs exposure to strain 17 improved their ability to mount an innate antiviral
324 immune response.

325 **Pulmonary exposure to strain 17 decreases the susceptibility of neonatal mice to RSV infection.**

326 Collectively, these *in vitro* results identify strain 17 as non cytotoxic strain capable of enhancing IFN-
327 I production and limiting RSV replication. We therefore evaluated whether pulmonary exposure to
328 strain 17 confers protection against RSV infection in neonatal mice. Additionally, we performed a
329 dose-response study to determine the minimal amount of strain 17 required to achieve its in vivo
330 immunomodulatory effect. Neonatal mice received three different amounts of strain 17 or PBS diluent
331 intranasally at 3- and 5-days old to modulate the neonatal lung mucosa before infection with RSV-
332 Luc at day 6 (**Fig. 5A**). Mice were euthanized 1 or 2 d.p.i. to assess viral replication in the nasal
333 cavities and lungs, as well as the associated immune response. As previously shown[9, 13], i.n. RSV-
334 Luc infection of neonatal mice led to rapid viral replication in the nasal cavity, reaching $1.42 \times 10^5 \pm$
335 0.38×10^5 and $0.89 \times 10^5 \pm 0.28 \times 10^5$ photons/mg at 1 and 2 d.p.i., respectively (**Fig. 5B**). In PBS-
336 treated neonates, lung replication was detectable at 1 d.p.i. ($1.02 \times 10^4 \pm 0.38 \times 10^4$ photons/mg) and
337 increased by 2 d.p.i. ($2.09 \times 10^4 \pm 0.32 \times 10^4$ photons/mg), confirmed by RSV *N gene* expression
338 (**Fig. 5C-D**). Strain 17 significantly reduced nasal viral replication at 1 d.p.i. at all doses (3-4-fold,
339 **Fig. 5B**), whereas only the 10^6 CFU dose significantly lowered lung replication ($0.098 \times 10^4 \pm 0.047$
340 $\times 10^4$ photons/mg, **Fig. 5C**). The 10^5 CFU dose showed delayed lung protection at 2 d.p.i., while the
341 10^3 CFU dose had no effect, indicating that upper airway protection requires lower doses, whereas
342 lung protection needs higher or delayed dosing (**Fig. 5B-D**). RSV infection in neonatal mouse lungs
343 induced low *IFN-I* gene expression at 1 d.p.i. (**Fig. 6A**), and led to a slight, non-significant, increase
344 in BAL cellularity between 1 and 2 d.p.i. (**Fig. 6B**), primarily due to neutrophil recruitment (**Fig. 6D**),
345 as previously shown[9, 12, 13]. In neonates treated with high doses of strain 17, *IFN-I gene* expressions,
346 and notably IFN-α, were increased at 1 d.p.i. (**Fig. 6A**), while total BAL cells (**Fig. 6B**) and
347 macrophages (**Fig. 6C**) remained unchanged. In contrast, neutrophil recruitment was significantly
348 enhanced from 1 to 2 d.p.i., with an ~8-fold increase at 2 d.p.i. in RSV-infected mice pre-treated with
349 the highest doses of strain 17 (**Fig. 6D**). Overall, these results demonstrate that neonatal exposure to
350 strain 17 enhances early innate immune responses, leading to reduced RSV replication, dose-
351 dependent protection of the lungs and a strong protective effect in the nasal cavity.

352 **Strain 17 limits RSV spread in a translational airway model.**

353 Finally, to validate the anti-RSV effect of strain 17 in a translational model, human primary airway
354 epithelial cells cultured at the air-liquid interface were pre-exposed to strain 17 and subsequently
355 infected with mCherry-expressing RSV to visualize cellular RSV replication (**Fig. 7A**). Without
356 bacterial pre-exposure, RSV replication was detectable at 48h post-infection, as shown by mCherry
357 fluorescence (**Fig. 7B**). In contrast, strain 17 exposure markedly reduced mCherry activity compared
358 to the control (**Fig. 7B-C**). No cytotoxicity was detected (**Fig. 7D**), and neither RSV exposure nor
359 treatment with strain 17 induced the production of cytokines (IL-6, TNF-α or IP-10, **Fig. Sup S4**) in

360 these experimental conditions. Type III interferons (IFN-λ) are produced by airway epithelial cells
361 infected with influenza virus earlier than IFN-I, helping to restrict viral spread without provoking
362 inflammation[34]. As expected, RSV infection induced IFN-λ production in epithelial cells (**Fig. 7E**).
363 Strain 17 alone did not induce IFN-λ and did not enhance the IFN-λ response to RSV infection; if
364 anything, it tended to reduce secretion. Overall, the effect of strain 17 is therefore unlikely to be
365 explained by an increase in IFN-λ. We then measured another antiviral factor, the antimicrobial
366 peptide human β-defensin 2, in epithelial cells (**Fig. 7F**). This cationic molecule, secreted by lung
367 epithelial cells, blocks RSV entry by destabilizing its envelope[35]. Strain 17 strongly induced β-
368 defensin 2 (2040 ± 571 pg/mL *vs* 65 ± 19 pg/mL in controls), whereas RSV alone triggered low levels
369 (120 ± 32 pg/mL). Thus, pre-exposure to strain 17 markedly reduced RSV propagation in a human
370 airway epithelium model without cytotoxicity, likely *via* enhanced β-defensin 2 secretion.
371

372 **Discussion**

373 The lung microbiota and its influence on RSV infection severity have recently been identified as
374 critical research areas in the fight against bronchiolitis in young children[23, 24 21]. While modulation of
375 the lung microbiota or metabolites appears to be a promising strategy for strengthening immune
376 defenses in adults[36, 37], the impact during the critical period of lung mucosal development and
377 susceptibility to RSV infection is yet unknown[28]. In this study, we demonstrated that the immune
378 responses of neonatal mice to RSV infection, as well as their long-term consequences, could be
379 favorably modulated by lung primo-colonizing bacterial strains given shortly after birth. In particular,
380 using complementary cellular and *in vivo* approaches, we identified a bacterial strain 17 (*E. coli*), that
381 promoted protective type 1 immune responses and limited RSV replication in both mouse neonatal
382 models and human epithelial cells.

383 We employed a PCLS-based screening platform from neonatal mice to assess cytokine responses
384 to a collection of primo-colonizing bacterial strains isolated from mouse neonatal lungs. This strain
385 collection encompasses major bacterial families, ranging from *Staphylococcus* to *Lactobacillus*.
386 While most *Lactobacillus* strains exhibited low immunostimulatory activity on neonatal PCLS, the
387 majority of *Staphylococcus* strains induced a pro-inflammatory cytokine profile. In contrast, strain
388 17, identified as *Escherichia coli*, uniquely induced a strong polarized type-1 cytokine response,
389 particularly IFN-γ and IL-12p70, without causing cytotoxicity, suggesting its potential to prime
390 antiviral immunity in the neonatal lung. However, strain 17 also induced the production of IL-9, a
391 cytokine linked to asthma and detected in airway aspirates from patients with severe bronchiolitis[38].
392 Its role in early-life pulmonary mucosa and RSV pathology remains poorly understood[39].
393 Interestingly, strain 17 also induced the secretion of IL-22, which is known to promote epithelial
394 barrier regeneration[40], and has a beneficial inhibitory effect on RSV infection has been demonstrated
395 in a neonatal mouse model[41]. Although cytokine accumulation during 24-hour PCLS-based screening
396 prevents the evaluation of secretion kinetics or autocrine effects, this approach nevertheless reveals
397 the broad potential of early-life lung primo-colonizing bacteria to induce immune stimulation and
398 polarization. Strain 17 differed markedly from the other lung primo-colonizing strains tested due to
399 its unique ability to limit RSV replication in both PCLS and a human airway epithelium model,
400 underscoring its translational relevance. It is interesting to note that strains taken individually may
401 display disease-specific immunobeneficial effects. Indeed, strain 24, previously shown to be
402 protective in a juvenile asthma model[19], had neither a protective nor a detrimental effect on RSV
403 replication in this study. These findings underscore the diverse immunomodulatory potential of
404 bacteria within the pulmonary microbiota. Functionally, the antiviral activity of strain 17 in human
405 epithelial cells appeared to be independent of IFN-λ and was associated with increased production of

406 β-defensin 2, a known host defense peptide capable of destabilizing the viral envelope, thereby
407 indirectly interfering with RSV entry and/or propagation[35]. Our study also demonstrated that strain
408 17 can prime anti-RSV immunity in neonatal AMs by enhancing their production of IFN-I. Thus,
409 strain 17 confers innate protective immunity to the lung mucosa in early-life.

410 Our *in vivo* studies confirmed the ability of strain 17 to reduce RSV replication in the upper and
411 lower respiratory tracts of neonatal mice. The degree of protection was dose-dependent and associated
412 with an induction of IFN-I expression, as well as increased neutrophil recruitment. The role of the
413 neutrophils recruited in strain 17-treated mice, with or without RSV infection, remains unclear,
414 particularly regarding their protective *versus* pathological effects in neonates[42]. Nevertheless, early-
415 life exposure to strain 17 mitigated long-term immunopathology upon re-exposure to RSV in
416 adulthood. Mice treated with strain 17 exhibited a relatively stable body weight curve with no major
417 alterations following viral reinfection, a shift toward type 1 immunity (increased IgG2a, decreased
418 IgG1), and reduced eosinophilic infiltration. These data indicate that early-life administration of strain
419 17 induces protective immunomodulation in the lung mucosa, mitigating the long-term consequences
420 of type 2 immune imprinting established by neonatal RSV infection. Although colonization was not
421 assessed, our study highlights the importance of dosing relative to the targeted respiratory region. For
422 instance, the instillation of 10^6 CFU into the lungs of a neonatal mouse represents a substantial
423 bacterial load compared to the naturally sparse neonatal lung microbiota[19]. Higher doses were
424 required to confer early protection in the lungs, whereas lower doses sufficed for the upper airways.
425 This likely reflects the larger tissue surface of the lungs that must be exposed to the bacteria, rather
426 than differences in microbiota density, which is already low in the pulmonary mucosa[43]. However,
427 before proposing this bacterial strain as a therapeutic candidate for early immunomodulation to
428 prevent acute and chronic RSV-related diseases, it is essential to elucidate the molecular pathways
429 underlying its immunostimulatory effects in both epithelial and immune cells. Future studies should
430 investigate whether the beneficial effects of strain 17 require live microorganisms, which colonize
431 tissues and are likely more effective than inert components to produce metabolites. Testing
432 conditioned supernatants could then clarify the contribution of bacterial metabolic activity, such as
433 acetate production *in vitro* (data not shown), a metabolite known to enhance antiviral responses in
434 AMs during RSV infection[44, 45]. Indeed, in an adult context, airway administration of *Lactobacillus*
435 or *Corynebacterium* strains[46, 47], or a standardized bacterial lysate derived from human respiratory
436 strains[48] is associated with improved resistance of mice to RSV challenge. Morever, higher acetate
437 levels boosts the IFN-β response of AMs and epithelial ISG expression, reducing viral load and
438 pulmonary inflammation in RSV-infected adult mice[44, 45]. It has been shown that *E. coli* probiotic
439 strains, can have both deleterious and beneficial effects on digestive health[49]. So, before exploiting a

such promising strain as a probiotic to enhance respiratory defenses, a global safety assessement is required.

Overall, this study reveals that the immune responses of neonatal mice to RSV infection, as well as their long-term consequences, can be favorably modulated by early-life lung-colonizing bacterial strains. These results reinforce the notion that the neonatal lung microbiota plays a key role in shaping pulmonary immune responses, and that its disruption, for example by antibiotics, can have profound and lasting effects on host immunity and respiratory vulnerability[50]. A recent study in pediatric RSV cohorts indicates that persistent respiratory symptoms during the convalescence phase are associated with disruptions to the respiratory microbiota[25]. It would be interesting to explore further the potential benefits of primo-colonizing strains during recovery.

451 **References**

452 1. Liu, L. *et al.* Global, regional, and national causes of under-5 mortality in 2000-15: an updated
453 systematic analysis with implications for the Sustainable Development Goals. *Lancet* **388**, 3027–
454 3035 (2016).
455 2. Zar, H.J. *et al.* Early-life respiratory syncytial virus disease and long-term respiratory health.
456 *Lancet Respir Med* **12**, 810–821 (2024).
457 3. Dieussaert, I. *et al.* RSV Prefusion F Protein-Based Maternal Vaccine - Preterm Birth and Other
458 Outcomes. *N Engl J Med* **390**, 1009–1021 (2024).
459 4. Mahase, E. FDA pauses all infant RSV vaccine trials after rise in severe illnesses. *BMJ* **387**,
460 q2852 (2024).
461 5. Cormier, S.A., You, D. & Honnegowda, S. The use of a neonatal mouse model to study
462 respiratory syncytial virus infections. *Expert Rev Anti Infect Ther* **8**, 1371–1380 (2010).
463 6. Morris, S.B. *et al.* Long-term alterations in lung epithelial cells after EL-RSV infection exacerbate
464 allergic responses through IL-1beta-induced pathways. *Mucosal Immunol* **17**, 1072–1088 (2024).
465 7. Malinczak, C.A. *et al.* Early-life pulmonary viral infection leads to long-term functional and lower
466 airway structural changes in the lungs. *Am J Physiol Lung Cell Mol Physiol* **326**, L280–L291 (2024).
467 8. Culley, F.J., Pollott, J. & Openshaw, P.J. Age at first viral infection determines the pattern of T
468 cell-mediated disease during reinfection in adulthood. *J Exp Med* **196**, 1381–1386 (2002).
469 9. Laubreton, D. *et al.* Regulatory B Lymphocytes Colonize the Respiratory Tract of Neonatal Mice
470 and Modulate Immune Responses of Alveolar Macrophages to RSV Infection in IL-10-dependant
471 Manner *Viruses* **12** (2020).
472 10. Hall, C.B., Douglas, R.G., Jr., Simons, R.L. & Geiman, J.M. Interferon production in children with
473 respiratory syncytial, influenza, and parainfluenza virus infections. *J Pediatr* **93**, 28–32 (1978).
474 11. Hijano, D.R. *et al.* Role of Type I Interferon (IFN) in the Respiratory Syncytial Virus (RSV)
475 Immune Response and Disease Severity. *Front Immunol* **10**, 566 (2019).
476 12. Cormier, S.A. *et al.* Limited type I interferons and plasmacytoid dendritic cells during neonatal
477 respiratory syncytial virus infection permit immunopathogenesis upon reinfection. *J Virol* **88**, 9350–
478 9360 (2014).
479 13. Remot, A. *et al.* Flt3 ligand improves the innate response to respiratory syncytial virus and limits
480 lung disease upon RSV reexposure in neonate mice. *Eur J Immunol* **46**, 874–884 (2016).
481 14. Torow, N., Marsland, B.J., Hornef, M.W. & Gollwitzer, E.S. Neonatal mucosal immunology.
482 *Mucosal Immunol* **10**, 5–17 (2017).
483 15. de Kleer, I.M. *et al.* Perinatal Activation of the Interleukin-33 Pathway Promotes Type 2 Immunity
484 in the Developing Lung. *Immunity* **45**, 1285–1298 (2016).
485 16. Saluzzo, S. *et al.* First-Breath-Induced Type 2 Pathways Shape the Lung Immune Environment.
486 *Cell Rep* **18**, 1893–1905 (2017).
487 17. Gollwitzer, E.S. *et al.* Lung microbiota promotes tolerance to allergens in neonates via PD-L1.
488 *Nat Med* **20**, 642–647 (2014).
489 18. Pattaroni, C., Marsland, B.J. & Harris, N.L. Early-Life Host-Microbial Interactions and Asthma
490 Development: A Lifelong Impact? *Immunol Rev* **330**, e70019 (2025).
491 19. Remot, A. *et al.* Bacteria isolated from lung modulate asthma susceptibility in mice. *ISME J* **11**,
492 1061–1074 (2017).
493 20. Pattaroni, C. *et al.* Bacterial communities co-develop with respiratory immunity early in life,
494 linking dysbiosis to systemic monocyte signature and wheezing. *Sci Adv* **11**, eadw1410 (2025).
495 21. Marquant, Q. *et al.* The microbiota plays a critical role in the reactivity of lung immune
496 components to innate ligands. *FASEB J* **35**, e21348 (2021).
497 22. de Steenhuijsen Piters, W.A.A. *et al.* Early-life viral infections are associated with
498 disadvantageous immune and microbiota profiles and recurrent respiratory infections. *Nat Microbiol*
499 **7**, 224–237 (2022).
500 23. Schippa, S. *et al.* Nasal Microbiota in RSV Bronchiolitis. *Microorganisms* **8** (2020).
501 24. Yagi, K., Asai, N., Huffnagle, G.B., Lukacs, N.W. & Fonseca, W. Early-Life Lung and Gut
502 Microbiota Development and Respiratory Syncytial Virus Infection. *Front Immunol* **13**, 877771
503 (2022).
504 25. Kristensen, M. *et al.* The respiratory microbiome is linked to the severity of RSV infections and
505 the persistence of symptoms in children. *Cell Rep Med* **5**, 101836 (2024).

506 26. Rosas-Salazar, C. *et al.* Nasopharyngeal Lactobacillus is associated with a reduced risk of
507 childhood wheezing illnesses following acute respiratory syncytial virus infection in infancy. *J Allergy*
508 *Clin Immunol* **142**, 1447–1456 e1449 (2018).
509 27. Bernard-Raichon, L. *et al.* A Pulmonary Lactobacillus murinus Strain Induces Th17 and
510 RORgammat(+) Regulatory T Cells and Reduces Lung Inflammation in Tuberculosis. *J Immunol*
511 **207**, 1857–1870 (2021).
512 28. de Steenhuijsen Piters, W.A.A., Binkowska, J. & Bogaert, D. Early Life Microbiota and
513 Respiratory Tract Infections. *Cell Host Microbe* **28**, 223–232 (2020).
514 29. Rameix-Welti, M.A. *et al.* Visualizing the replication of respiratory syncytial virus in cells and in
515 living mice. *Nat Commun* **5**, 5104 (2014).
516 30. Descamps, D. *et al.* Toll-like receptor 5 (TLR5), IL-1beta secretion, and asparagine
517 endopeptidase are critical factors for alveolar macrophage phagocytosis and bacterial killing. *Proc*
518 *Natl Acad Sci U S A* **109**, 1619–1624 (2012).
519 31. Drajac, C. *et al.* Control of IFN-I responses by the aminopeptidase IRAP in neonatal C57BL/6
520 alveolar macrophages during RSV infection. *Mucosal Immunol* **14**, 949–962 (2021).
521 32. Liu, G. *et al.* Use of precision cut lung slices as a translational model for the study of lung biology.
522 *Respir Res* **20**, 162 (2019).
523 33. Makris, S., Bajorek, M., Culley, F.J., Goritzka, M. & Johansson, C. Alveolar Macrophages Can
524 Control Respiratory Syncytial Virus Infection in the Absence of Type I Interferons. *J Innate Immun* **8**,
525 452–463 (2016).
526 34. Galani, I.E. *et al.* Interferon-lambda Mediates Non-redundant Front-Line Antiviral Protection
527 against Influenza Virus Infection without Compromising Host Fitness. *Immunity* **46**, 875–890 e876
528 (2017).
529 35. Kota, S. *et al.* Role of human beta-defensin-2 during tumor necrosis factor-alpha/NF-kappaB-
530 mediated innate antiviral response against human respiratory syncytial virus. *J Biol Chem* **283**,
531 22417–22429 (2008).
532 36. Drajac, C., Laubreton, D., Riffault, S. & Descamps, D. Pulmonary Susceptibility of Neonates to
533 Respiratory Syncytial Virus Infection: A Problem of Innate Immunity? *J Immunol Res* **2017**, 8734504
534 (2017).
535 37. Fonseca, W., Lukacs, N.W. & Ptaschinski, C. Factors Affecting the Immunity to Respiratory
536 Syncytial Virus: From Epigenetics to Microbiome. *Front Immunol* **9**, 226 (2018).
537 38. McNamara, P.S. *et al.* Interleukin 9 production in the lungs of infants with severe respiratory
538 syncytial virus bronchiolitis. *Lancet* **363**, 1031–1037 (2004).
539 39. Dodd, J.S. *et al.* IL-9 regulates pathology during primary and memory responses to respiratory
540 syncytial virus infection. *J Immunol* **183**, 7006–7013 (2009).
541 40. Dean, L.S. *et al.* I don't know about you, but I'm feeling IL-22. *Cytokine Growth Factor Rev* **80**,
542 1–11 (2024).
543 41. Das, S. *et al.* Interleukin-22 Inhibits Respiratory Syncytial Virus Production by Blocking Virus-
544 Mediated Subversion of Cellular Autophagy. *iScience* **23**, 101256 (2020).
545 42. Tahamtan, A. *et al.* Neutrophils in respiratory syncytial virus infection: From harmful effects to
546 therapeutic opportunities. *Br J Pharmacol* **178**, 515–530 (2021).
547 43. Ozcam, M. & Lynch, S.V. The gut-airway microbiome axis in health and respiratory diseases.
548 *Nat Rev Microbiol* **22**, 492–506 (2024).
549 44. Antunes, K.H. *et al.* Microbiota-derived acetate protects against respiratory syncytial virus
550 infection through a GPR43-type 1 interferon response. *Nat Commun* **10**, 3273 (2019).
551 45. Ji, J.J. *et al.* Probiotics protect against RSV infection by modulating the microbiota-alveolar-
552 macrophage axis. *Acta Pharmacol Sin* **42**, 1630–1641 (2021).
553 46. Villena, J. *et al.* Orally administered Lactobacillus rhamnosus modulates the respiratory immune
554 response triggered by the viral pathogen-associated molecular pattern poly(I:C). *BMC Immunol* **13**,
555 53 (2012).
556 47. Kanmani, P. *et al.* Respiratory Commensal Bacteria Corynebacterium pseudodiphtheriticum
557 Improves Resistance of Infant Mice to Respiratory Syncytial Virus and Streptococcus pneumoniae
558 Superinfection. *Front Microbiol* **8**, 1613 (2017).
559 48. Antunes, K.H. *et al.* Airway Administration of Bacterial Lysate OM-85 Protects Mice Against
560 Respiratory Syncytial Virus Infection. *Front Immunol* **13**, 867022 (2022).

561 49. Nougayrede, J.P. *et al.* A Toxic Friend: Genotoxic and Mutagenic Activity of the Probiotic Strain
562 Escherichia coli Nissle 1917. *mSphere* **6**, e0062421 (2021).
563 50. Perdijk, O. *et al.* Antibiotic-driven dysbiosis in early life disrupts indole-3-propionic acid
564 production and exacerbates allergic airway inflammation in adulthood. *Immunity* **57**, 1939–1954
565 e1937 (2024).
566
567

568 **Figure legends (max 10 avec les tableaux)**

569 **Fig. 1:** Cytokine production by precision-cut lung slices (PCLS) from neonatal mice varies in
570 response to exposure to lung primo-colonizing bacteria. **A**. Experimental design. The lungs from 6-
571 day-old mice were isolated and cut with a Krumdieck tissue slicer to obtain PCLS. They were next
572 exposed to bacteria (50 CFU/well) or cultured in medium control. Supernatants were collected 16h
573 after stimulation with bacterial strains and PCLS were lysed. **B**. Secretion of cytokines associated
574 with type 1 immune response (IFN-β, IL-12p70). Results are expressed as mean ± SEM and represent
575 a pool of five independent experiments (n = 2-5 biological replicate samples/condition). *$P < 0.05$,
576 **$P < 0.01$, ***$P < 0.001$ and ****$P < 0.0001$ between the control medium and the strain-exposed
577 condition (ANOVA, Kruskal-Wallis test followed by Dunn's post-hoc test). **C**. The heat map
578 illustrates the fold-change (FC) of cytokine production induced after bacterial exposure. For each
579 strain and cytokine secretion, the FC were calculated using the following formula: FC = (average of
580 the stimulated conditions)/(average of the control conditions). FC were entered into Morpheus online
581 software (Broad Institute) to obtain the heatmaps.
582
583

584 **Fig. 2 :** Early-life airway administration of strain 17 attenuates the long-term pulmonary
585 consequences of neonatal RSV infection during reinfection in adulthood. **A**. Experimental design.
586 Three-day-old mice were treated intranasally with bacterium 17 (10^6 CFU, i.n., 10 µL) or PBS vehicle
587 at days 3, 5, 8, and 10 days of age. At 6 days old, mice were infected intranasally with RSV-A2 (2.3
588 × 10^4 PFU in 10 µL), followed by a second infection with RSV-A2 (2.3 × 10^5 PFU in 100 µL, i.n.) at
589 8 weeks of age. Mice were euthanized at 7, 9 or 14 days post-reinfection (d.p.i.) to assess cellular
590 infiltration in the BALs and blood was collected. **B**. Weight evolution after the second infection.
591 Results are expressed as mean ± SEM and presented as a percentage of the starting weight (n = 4 per
592 group). **C-D**. Anti-RSV antibody assays. Serum was used to quantify anti-RSV IgG1 (**C**) or IgG2a
593 (**D**) antibodies by ELISA. Results are expressed as the mean ± SEM (n = 4-5 per group). *$P < 0.05$,
594 **$P < 0.01$, Mann-Whitney test. **E-F**. The infiltration of eosinophils in BALs was assessed by May-
595 Grünwald-Giemsa staining at 7 or 9 d.p.i.. Results are expressed as mean ± SEM. Data are
596 representative of two independent experiments (n = 5-9 per group). *$P < 0.05$, **$P < 0.01$, Mann-
597 Whitney test.
598

599 **Fig. 3:** RSV replication in neonatal PCLS is differentially affected by primo-colonizing commensal
600 bacteria. **A**. Experimental design. The lungs from 6-day-old mice were isolated and cut with a
601 Krumdieck tissue slicer to obtain PCLS. They were next exposed to strains 16, 17, 24 or 25 (50

602 CFU/well) or cultured in control medium. PCLS were infected with RSV expressing luciferase (RSV-
603 Luc, 7.187 x 10^4 PFU/well) or mock control (-) 3h after bacterial stimulation. Supernatants were
604 collected 16h after bacterial stimulation and PCLS were lysed. **B**. Cytotoxicity observed in PCLS was
605 measured by LDH activity assay. Results are expressed as the mean ± SEM and represent a pool of
606 four independent experiments (n = 5-18 per group in simplicate). **C**. RSV-Luc replication was
607 assessed by measuring luciferase activity in lysates of PCLS exposed or unexposed to strains. Results
608 are expressed as mean ± SEM and represent a pool of four independent experiments (n = 6-21 per
609 group in duplicate). *$P < 0.05$ and ****$P < 0.0001$ between the control medium or the strain-exposed
610 condition (ANOVA, Kruskal-Wallis test followed by Dunn's post-hoc test).
611
612 **Fig. 4:** Cytokines and type I interferon (IFN-I) production by RSV-infected alveolar macrophages
613 (AMs) from neonatal mice is enhanced in response to exposure to strain 17. **A**. Experimental design.
614 AMs isolated from BAL of neonatal mice were exposed to strain 17 (50 CFU/well) or cultured in
615 medium control. AMs were infected with rRSV-long (MOI = 5) 3h after bacterial stimulation.
616 Supernatants were collected 16h after bacterial stimulation and AMs were lysed. The production of
617 pro-inflammatory cytokines (IL-6 and TNF-α, **B**) and IFN-I (IFN-α and IFN-β, **C**) was measured in
618 supernatants using multiplex immunoassay. Data are representative of two independent experiments.
619 Means ± SEM are represented. *$P < 0.05$, **$P < 0.01$, ***$P < 0.001$ and ****$P < 0.0001$ (2way
620 ANOVA with Tukey's multiple comparisons test).
621
622 **Fig. 5:** Early-life airway administration of strain 17 restricts RSV replication in neonatal mice. **A**.
623 Experimental design. Neonatal mice were treated with different quantities of strain 17 (10^3, 10^5 or
624 10^6 CFU) or PBS vehicle at 3 and 5-days old (i.n., 10 µL). At 6-days old, mice were infected with
625 RSV-Luc (7.2 x 10^4 PFU, 10 µL, i.n) and were euthanized at 1 d.p.i or 2 d.p.i. to assess viral
626 replication by luciferase activity assay in the lysats of nasal cavities (**B**) and lungs (**C**). **D**. The viral
627 replication was evaluated by quantification of the RSV *N gene* expression. The level of expression
628 was calculated by the formula $2^{-\Delta Cq}$ with $\Delta CQ = Cq_{N\ gene} - Cq_{reference\ genes}$. Results are expressed as mean
629 ± SEM. Data are representative of two independent experiment (n = 5-8 per group). *$P < 0.05$, **P
630 < 0.01, ***$P < 0.001$, Mann-Whitney test.
631
632 **Fig. 6:** Early-life airway administration of strain 17 enhances neonatal pulmonary immunity against
633 RSV. Neonatal mice were treated with different quantities of strain 17 (10^3, 10^5 or 10^6 CFU) or PBS
634 vehicle at 3 and 5-days old (i.n., 10 µL). At 6 days old, mice were infected with RSV-Luc (7.2 x 10^4
635 PFU, 10 µL, i.n) and were euthanized at 1 or 2 d.p.i. **A**. *IFN-I gene* expression was measured by qRT-

636 PCR in lung lysates at 1 d.p.i.. Gene expression levels were calculated using the $2^{-\Delta Cq}$ method, with
637 Cq values normalized to housekeeping genes. **B**. Cell counts were performed on BAL samples at 1
638 or 2 d.p.i.. Cell infiltration in BALs was assessed by May-Grünwald-Giemsa staining to identify and
639 differentiate macrophages (**C**) and polynuclear neutrophils (**D**) at 1 or 2 d.p.i.. Results are expressed
640 as mean ± SEM. Data are representative of two independent experiments (n = 5-8 per group). *P <
641 0.05, **P < 0.01, Mann-Whitney test.
642
643 **Fig. 7:** RSV replication in human primary airway epithelial cells is reduced by the pre-exposure to
644 strain 17. **A**. Experimental design. Human primary bronchial epithelial cells cultured at the air liquid
645 interface (MucilAir™) were first exposed to strain 17 (10^3 CFU/well) for 3h, followed by RSV
646 expressing mCherry (RSV-mCherry, MOI = 0.1) infection or an incubation with mock for a further
647 3h. Supernatants and cell lysates were collected 48h after incubation. RSV replication was evaluated
648 by detecting mCherry using microscopy (**B**, three images representative of six inserts) or a
649 fluorescence plate reader (**C**). Results are expressed as the mean fluorescence intensity (MFI)
650 observed in lysats of RSV-mCherry-infected cells, after subtraction of the background MFI from
651 mock-infected controls (± SEM), and represent a pool of two independent experiments (n = 3 inserts
652 per group per experiment, **P < 0.01, Mann-Whitney test). **D**. Cytotoxicity observed in MucilAir™
653 was measured by LDH activity assay. Results are expressed as mean ± SEM. **E**. Bioactive IFN-λ was
654 evaluated by measuring the response of HEK-Blue™ IFN-λ cells to the supernatants. SEAP activity
655 was assessed using QUANTI-Blue™ Solution. The optical density (OD) at 630 nm is shown as mean
656 ± SEM. **F**. β-defensin 2 secretion in supernatants was evaluated by ELISA. **E-F**. Data represent a
657 pool of two independent experiments (n = 9 inserts per group, ***P < 0.001, ****P < 0.0001, 2way
658 ANOVA with Tukey's multiple comparisons test).
659
660
661
662
663 **<u>Supplemental figure legend</u>**

664 **Supplemental Fig. 1: Cytokines production of precision-cut lung slices (PCLS) from neonatal**
665 **mice in response to exposure to lung primo-colonizing bacteria.** The lungs from 6-day-old mice
666 were isolated and cut with a Krumdieck tissue slicer to obtain PCLS. They were then exposed to
667 bacteria (50 CFU/well) or cultured in control medium. Supernatants were collected 16h after
668 stimulation with bacterial strains or PBS, and cytokine production was assessed using the 15-plex
669 Mouse ProcartaPlex™ immunoassay. **A**. Cytotoxicity observed in PCLS after bacterial exposure was

670 measured by LDH activity assay. **B**. Pro-inflammatory cytokine secretion (GM-CSF, IL-6, IL-1β,
671 TNF-α). **C**. Cytokine associated with type 1 immune response (IL-18). **D**. Cytokines associated with
672 type 2 immune response (IL-4, IL-5, IL-10, IL-13). **E**. Cytokines associated with type 17/22/9
673 immune response (IL-17A, IL-22, IL-9). **F**. Secretion of IL-2 associated with cell proliferation
674 response. Results are expressed as mean ± SEM and represent a pool of five independent experiments
675 (n = 2-5 biological replicate samples/condition). *$P < 0.05$, **$P < 0.01$, ***$P < 0.001$, and ****$P <$
676 0.0001 between the control medium and the bacteria-exposed condition (ANOVA, Kruskal-Wallis
677 test followed by Dunn's post-hoc test).
678
679 **Supplemental Fig. 2: Bronchoalveolar cellular response to intranasal exposure to strain 17 in**
680 **neonatal mice. A.** Experimental design. Three-day-old mice were treated intranasally with strain 17
681 (10^6 CFU, i.n., 10 µL) or PBS vehicle on days 3 and 5 of age. At day 7 and 8 of age, mice were
682 euthanized and BAL were collected. **B**. Total cell counts in BAL samples. Cellular composition in
683 BAL was assessed by May-Grünwald-Giemsa staining to identify and differentiate macrophages (**C**)
684 and neutrophils (**D**). Results are expressed as mean ± SEM (n = 3 per group). *$P < 0.05$ between the
685 PBS- and the bacteria-exposed condition (ANOVA, Kruskal-Wallis test followed by Dunn's post-
686 hoc test).
687
688 **Supplemental Fig. 3: Early-life airway delivery of strain 17 prevents weight loss during RSV**
689 **reinfection in adulthood and shapes the adaptive antibody response. A.** Experimental design.
690 Three-day-old mice were treated intranasally with strain 17 (10^6 CFU, i.n., 10 µL) or PBS vehicle at
691 days 3, 5, 8, and 10 of age. On postnatal day 6, mice were infected intranasally with RSV-A2 ($2.3 \times$
692 10^4 PFU in 10 µL), followed by a second infection with RSV-A2 (2.3×10^5 PFU in 100 µL, i.n.) at 8
693 weeks of age. **B-E.** Mice were euthanized at 7 or 9 d.p.i. to assess cell infiltration in the
694 bronchoalveolar lavage (BAL). **B**. Total cell counts in BAL. Cell infiltration in BAL was assessed by
695 May-Grünwald-Giemsa staining to identify and differentiate macrophages (**C**), neutrophils (**D**), and
696 lymphocytes (**E**) at 7 or 9 d.p.i.. Results are expressed as mean ± SEM. Data are representative of
697 two independent experiments (n = 5-9 per group). *$P < 0.05$, **$P < 0.01$, Mann-Whitney test.
698
699 **Supplemental Fig. 4: Cytokine response to RSV infection in primary human airway cells with**
700 **or without strain 17 pre-exposure.** Human primary bronchial epithelial cells cultured at the air-
701 liquid interface (MucilAir™) were first exposed to strain 17 (10^3 CFU/well) for 3h, followed by RSV
702 expressing mCherry (RSV-mCherry, MOI = 0.1) infection or incubation with mock. Basal medium

703 and cell lysates were collected 48h after incubation. IL-6, TNF-α or IP-10 concentrations in basal
704 medium were assessed using Luminex immunoassay. Means ± SEM are represented.
705
706
707
708
709

Early-Life Commensal Lung Bacteria Shape Immune Responses and RSV Susceptibility in mice

Figures

Figure 1

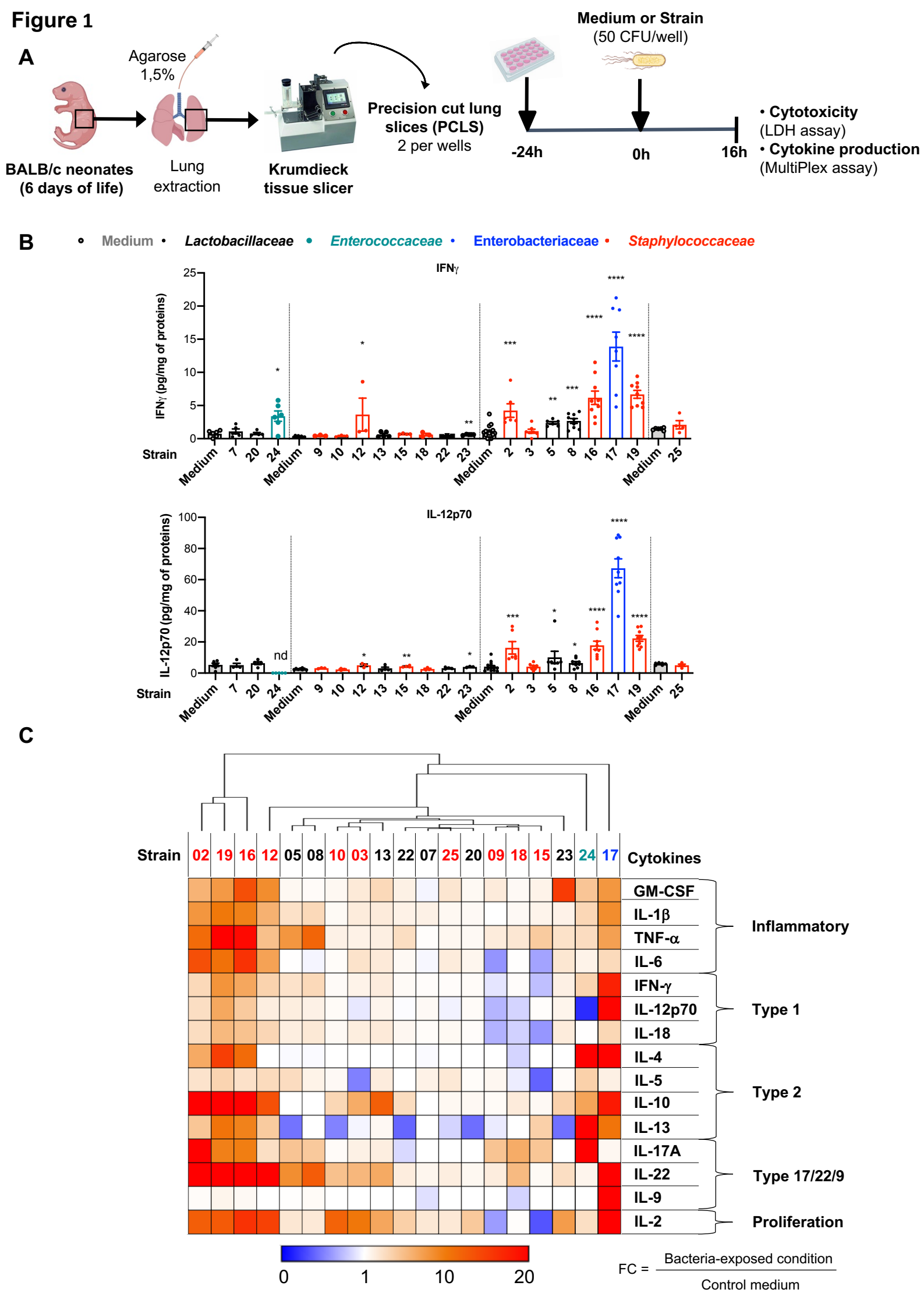
A
Agarose 1,5%
BALB/c neonates (6 days of life)
Lung extraction
Krumdieck tissue slicer
Precision cut lung slices (PCLS)
2 per wells
Medium or Strain
(50 CFU/well)
-24h
0h
16h
• Cytotoxicity
(LDH assay)
• Cytokine production
(MultiPlex assay)
B
Medium
Lactobacillaceae
Enterococcaceae
Enterobacteriaceae
Staphylococcaceae
IFNγ
IFNγ (pg/mg of proteins)
IL-12p70
IL-12p70 (pg/mg of proteins)
nd
Strain
Medium 7 20 24 Medium 9 10 12 13 15 18 22 23 Medium 2 3 5 8 16 17 19 Medium 25
C
Strain
02 19 16 12 05 08 10 03 13 22 07 25 20 09 18 15 23 24 17
Cytokines
GM-CSF
IL-1β
TNF-α
IL-6
IFN-γ
IL-12p70
IL-18
IL-4
IL-5
IL-10
IL-13
IL-17A
IL-22
IL-9
IL-2
Inflammatory
Type 1
Type 2
Type 17/22/9
Proliferation
0 1 10 20
FC = Bacteria-exposed condition / Control medium

Figure 2

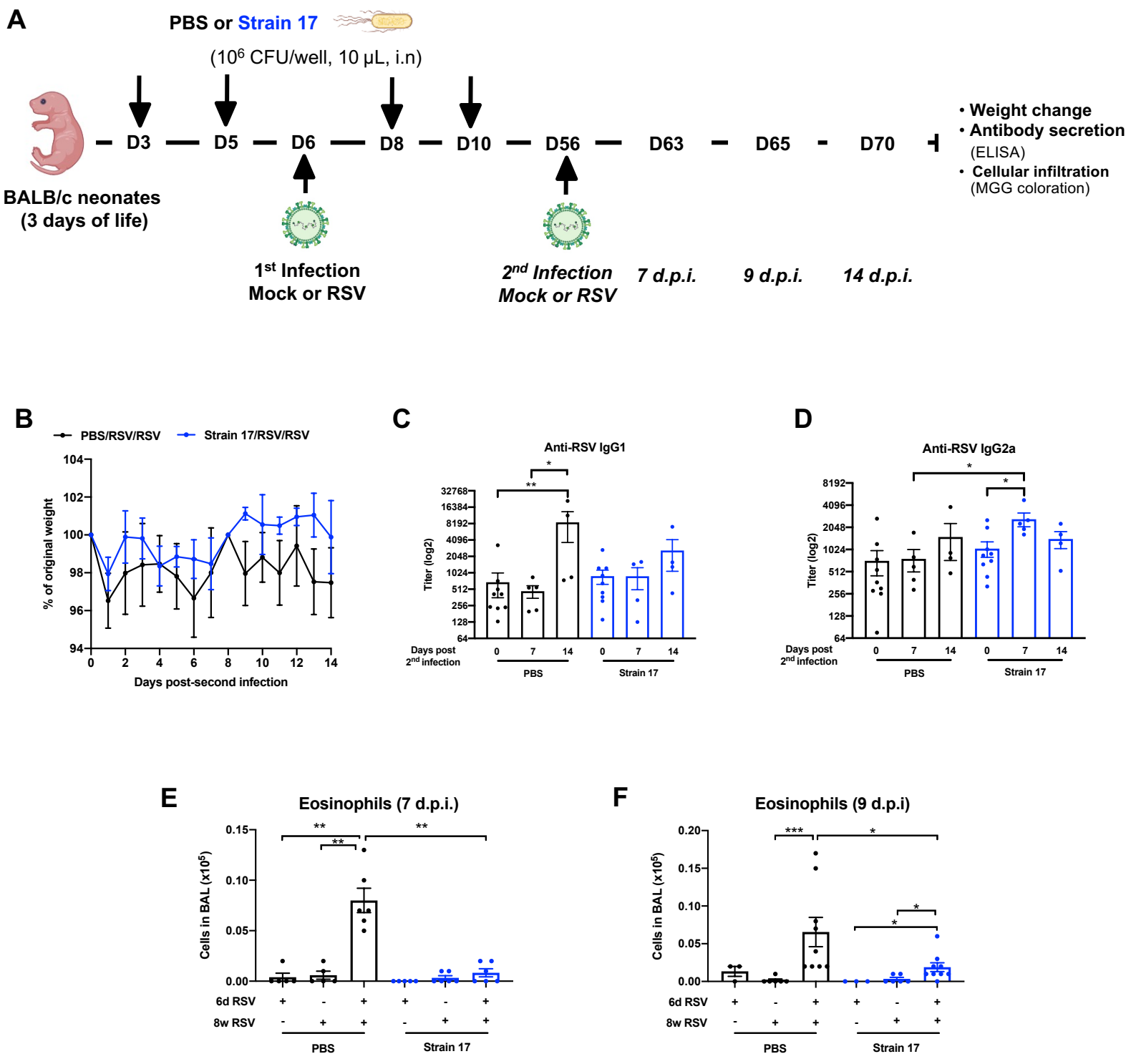
A
PBS or Strain 17
(10^6 CFU/well, 10 µL, i.n)
BALB/c neonates
(3 days of life)
D3
D5
D6
D8
D10
D56
D63
D65
D70
• Weight change
• Antibody secretion (ELISA)
• Cellular infiltration (MGG coloration)
1st Infection
Mock or RSV
2nd Infection
Mock or RSV
7 d.p.i.
9 d.p.i.
14 d.p.i.
B
PBS/RSV/RSV
Strain 17/RSV/RSV
% of original weight
Days post-second infection
C
Anti-RSV IgG1
Titer (log2)
Days post 2nd infection
PBS
Strain 17
D
Anti-RSV IgG2a
Titer (log2)
Days post 2nd infection
PBS
Strain 17
E
Eosinophils (7 d.p.i.)
Cells in BAL (x10^5)
6d RSV
8w RSV
PBS
Strain 17
F
Eosinophils (9 d.p.i)
Cells in BAL (x10^5)
6d RSV
8w RSV
PBS
Strain 17

Figure 3

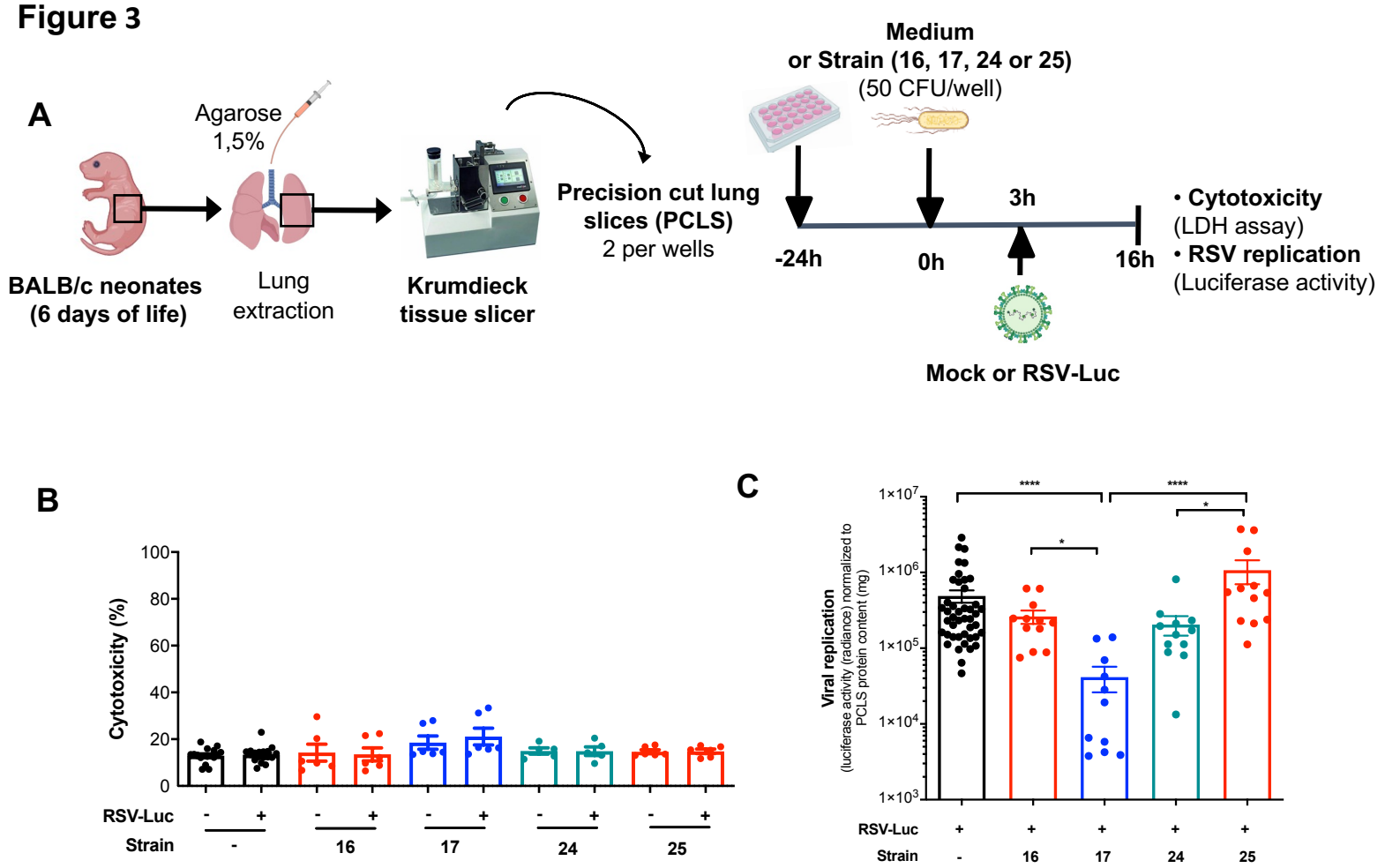
A
Agarose
1,5%
BALB/c neonates
(6 days of life)
Lung
extraction
Krumdieck
tissue slicer
Precision cut lung
slices (PCLS)
2 per wells
Medium
or Strain (16, 17, 24 or 25)
(50 CFU/well)
-24h
0h
3h
16h
Mock or RSV-Luc
• Cytotoxicity
(LDH assay)
• RSV replication
(Luciferase activity)
B
Cytotoxicity (%)
100
80
60
40
20
0
RSV-Luc
Strain
16
17
24
25
C
Viral replication
(luciferase activity (radiance) normalized to
PCLS protein content (mg)
1×10^7
1×10^6
1×10^5
1×10^4
1×10^3
****
*
RSV-Luc
Strain
16
17
24
25

Figure 4

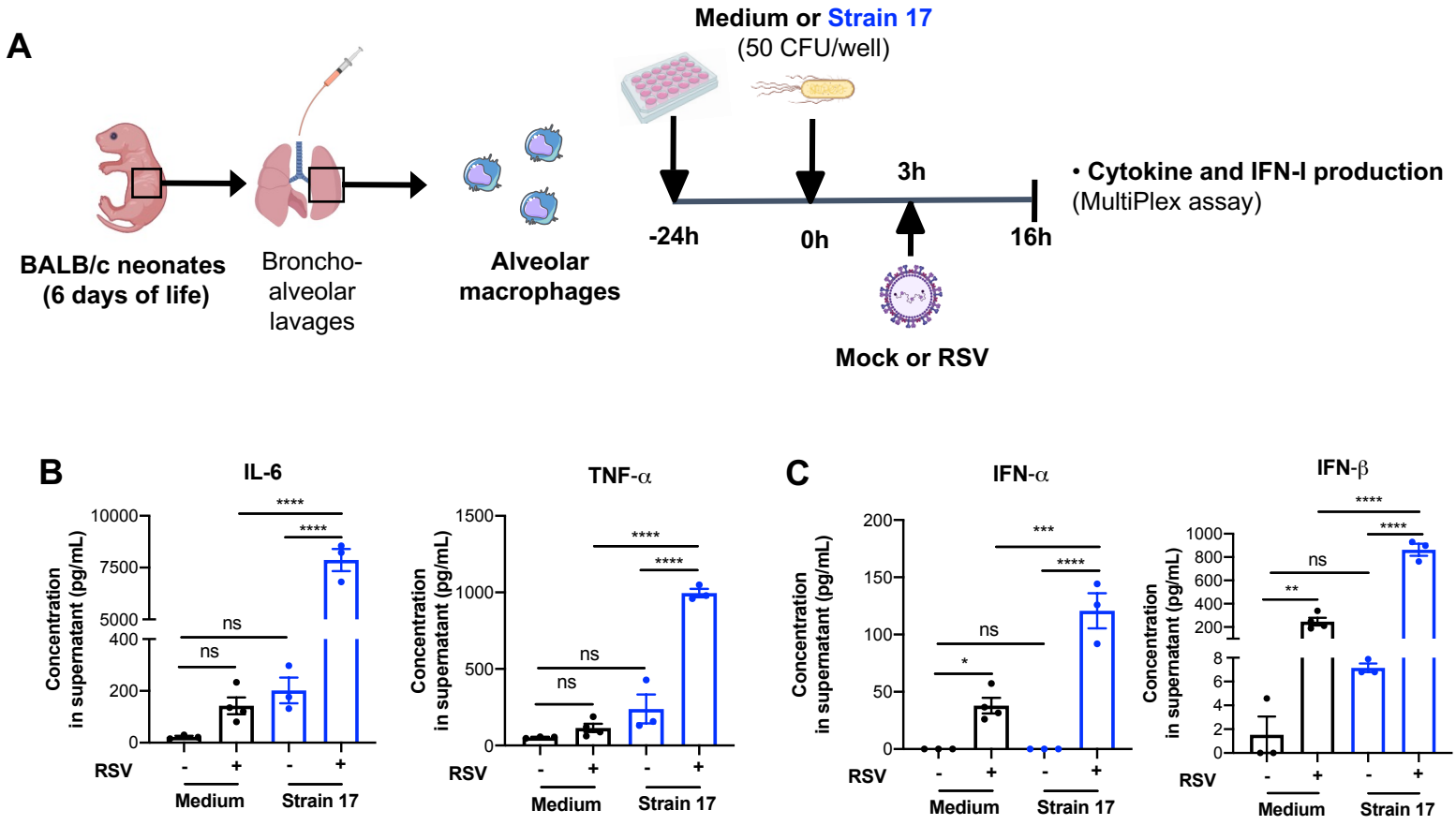
A
BALB/c neonates
(6 days of life)
Broncho-
alveolar
lavages
Alveolar
macrophages
Medium or Strain 17
(50 CFU/well)
-24h
0h
3h
16h
Mock or RSV
• Cytokine and IFN-I production
(MultiPlex assay)
B
IL-6
TNF-α
C
IFN-α
IFN-β
Concentration
in supernatant (pg/mL)
RSV
Medium
Strain 17
ns
****
***
*
**

Figure 5

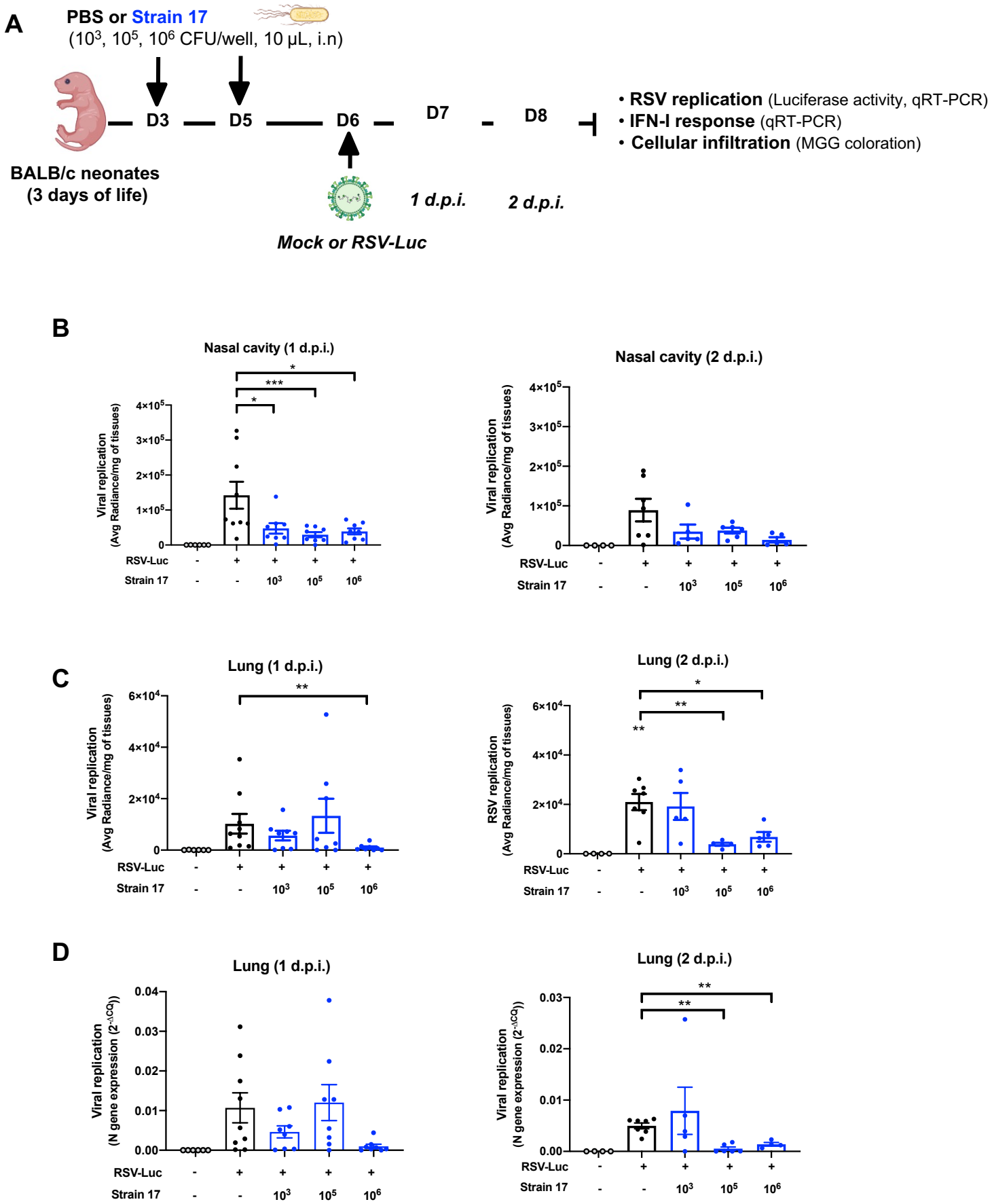
A
PBS or Strain 17
(10³, 10⁵, 10⁶ CFU/well, 10 µL, i.n)
BALB/c neonates
(3 days of life)
D3
D5
D6
D7
D8
1 d.p.i.
2 d.p.i.
Mock or RSV-Luc
• RSV replication (Luciferase activity, qRT-PCR)
• IFN-I response (qRT-PCR)
• Cellular infiltration (MGG coloration)
B
Nasal cavity (1 d.p.i.)
Nasal cavity (2 d.p.i.)
Viral replication
(Avg Radiance/mg of tissues)
C
Lung (1 d.p.i.)
Lung (2 d.p.i.)
RSV replication
(Avg Radiance/mg of tissues)
D
Viral replication
(N gene expression (2^-ΔCQ))
RSV-Luc
Strain 17

Figure 6

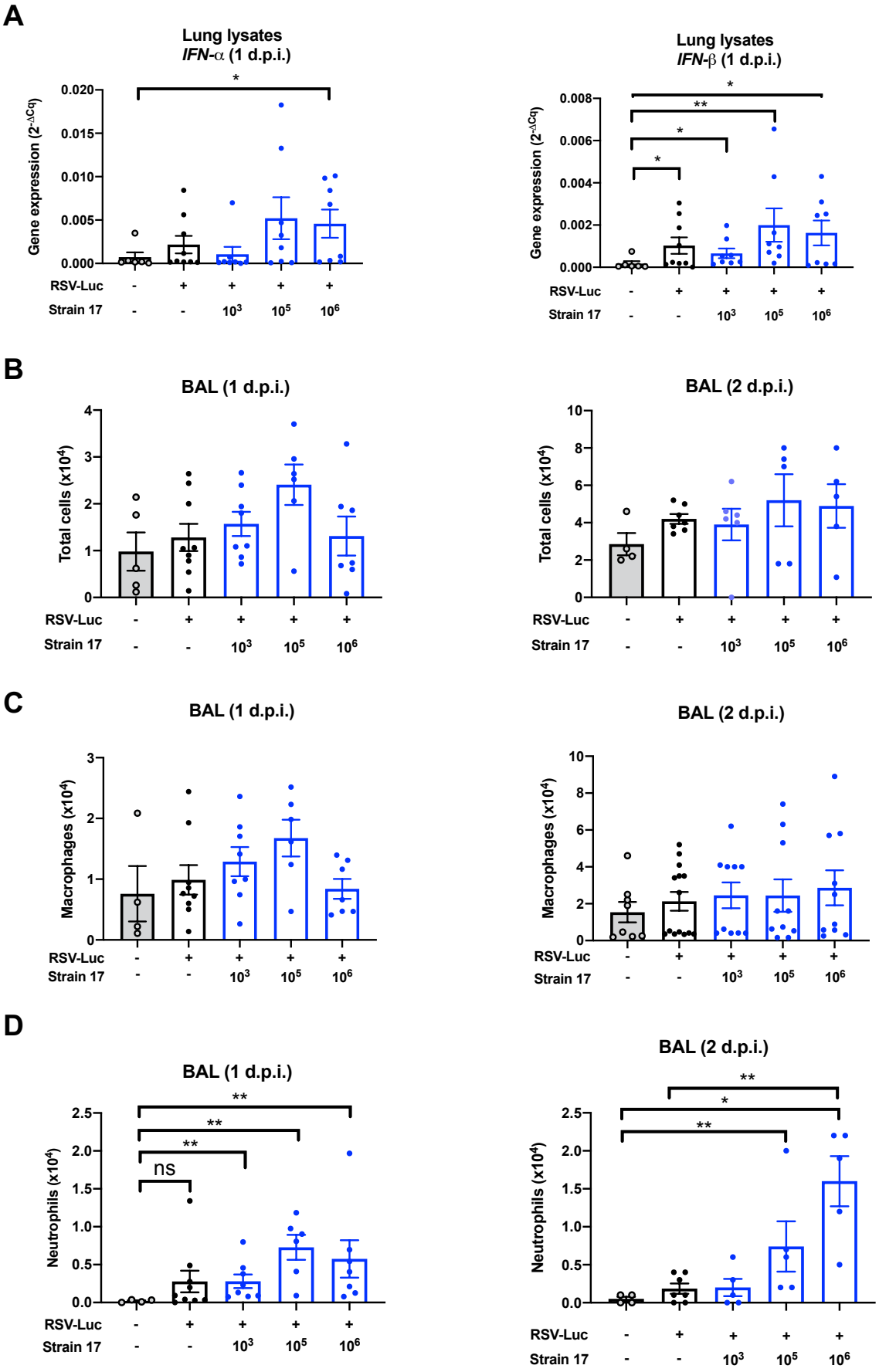
A
Lung lysates
IFN-α (1 d.p.i.)
Gene expression (2^-ΔCq)
0.020
0.015
0.010
0.005
0.000
*
RSV-Luc - + + + +
Strain 17 - - 10^3 10^5 10^6
Lung lysates
IFN-β (1 d.p.i.)
Gene expression (2^-ΔCq)
0.008
0.006
0.004
0.002
0.000
*
**
*
*
RSV-Luc - + + + +
Strain 17 - - 10^3 10^5 10^6
B
BAL (1 d.p.i.)
Total cells (x10^4)
4
3
2
1
0
RSV-Luc - + + + +
Strain 17 - - 10^3 10^5 10^6
BAL (2 d.p.i.)
Total cells (x10^4)
10
8
6
4
2
0
RSV-Luc - + + + +
Strain 17 - - 10^3 10^5 10^6
C
BAL (1 d.p.i.)
Macrophages (x10^4)
3
2
1
0
RSV-Luc - + + + +
Strain 17 - - 10^3 10^5 10^6
BAL (2 d.p.i.)
Macrophages (x10^4)
10
8
6
4
2
0
RSV-Luc - + + + +
Strain 17 - - 10^3 10^5 10^6
D
BAL (1 d.p.i.)
Neutrophils (x10^4)
2.5
2.0
1.5
1.0
0.5
0.0
**
**
**
ns
RSV-Luc - + + + +
Strain 17 - - 10^3 10^5 10^6
BAL (2 d.p.i.)
Neutrophils (x10^4)
2.5
2.0
1.5
1.0
0.5
0.0
**
*
**
RSV-Luc - + + + +
Strain 17 - - 10^3 10^5 10^6

Figure 7

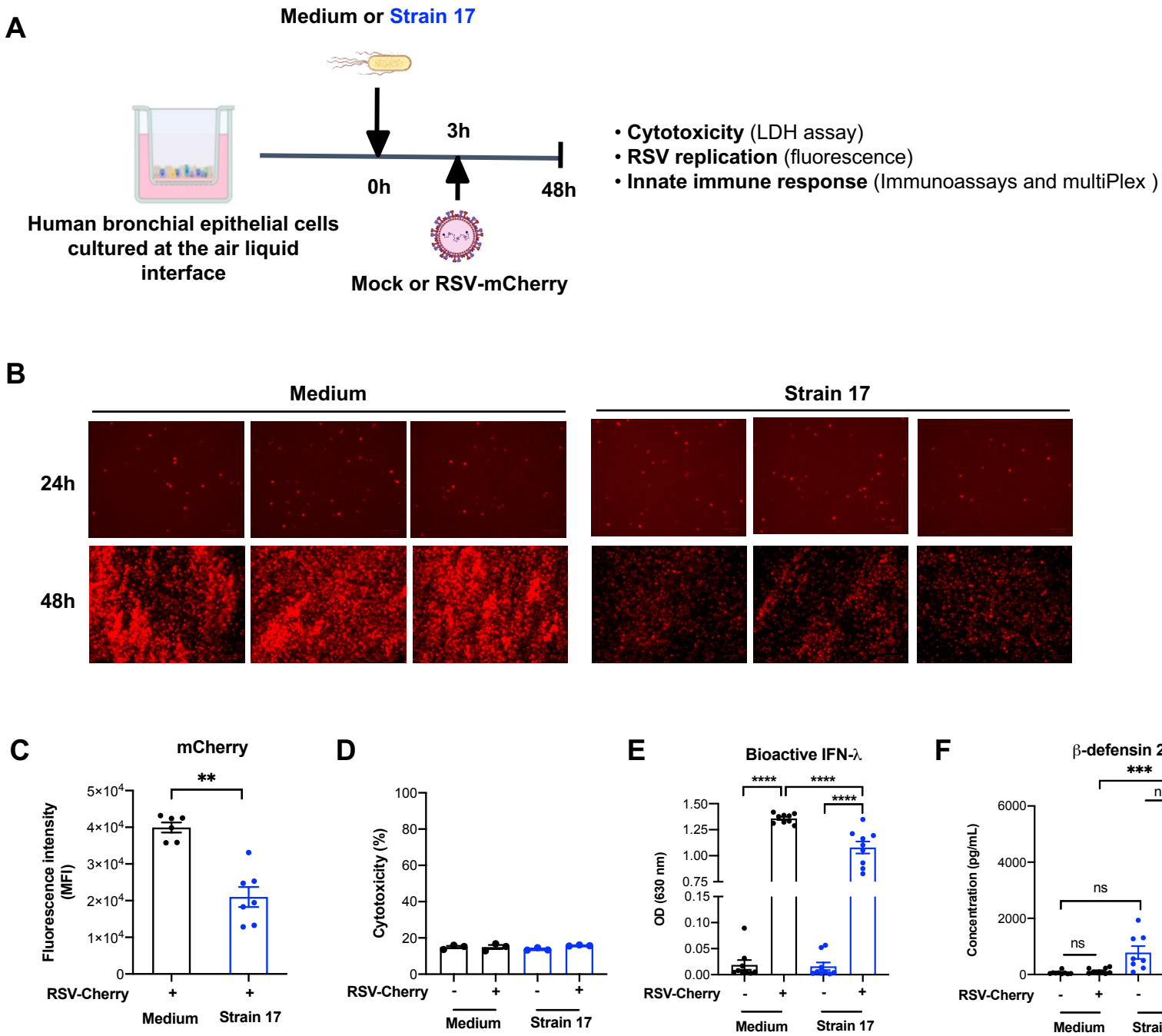
A
Medium or Strain 17
3h
0h
48h
Human bronchial epithelial cells cultured at the air liquid interface
Mock or RSV-mCherry
• Cytotoxicity (LDH assay)
• RSV replication (fluorescence)
• Innate immune response (Immunoassays and multiPlex)
B
Medium
Strain 17
24h
48h
C
mCherry
Fluorescence intensity (MFI)
5×10^4
4×10^4
3×10^4
2×10^4
1×10^4
0
**
RSV-Cherry
+
+
Medium
Strain 17
D
Cytotoxicity (%)
100
80
60
40
20
0
RSV-Cherry
-
+
-
+
Medium
Strain 17
E
Bioactive IFN-λ
OD (630 nm)
1.50
1.25
1.00
0.75
0.15
0.10
0.05
0.00
****
****
****
RSV-Cherry
-
+
-
+
Medium
Strain 17
F
β-defensin 2
Concentration (pg/mL)
6000
4000
2000
0
***
ns
ns
ns
RSV-Cherry
-
+
-
+
Medium
Strain 17